Gazi Üniversitesi
Fen Bilimleri Dergisi
PART C: TASARIM VE TEKNOLOJİ

Gazi University
Journal of Science
PART C: DESIGN AND TECHNOLOGY

GU J Sci, Part C, 13(X): XX-XX (2025)

Multi-Focal Diffractive Lens by Apodized Phase Photon Sieves

Ahmet ÜNAL[1*]

[1]*Middle East Technical University, Department of Electrical and Electronics Engineering, Ankara, Turkey*

Article Info

Research article
Received: 30/09/2024
Revision: 16/03/2025
Accepted: 24/03/2025

Keywords

Diffractive Optical Elements
Phase Fresnel Zone Plates
Multilevel Diffractive Lens
Point Spread Function
EMI Shielding

Makale Bilgisi

Araştırma makalesi
Başvuru: 30/09/2024
Düzeltme: 16/03/2025
Kabul: 24/03/2025

Anahtar Kelimeler

Kırınımlı Optik Eleman
Faz Fresnel Bölge Plakaları
Çok Seviyeli Kırınımlı Lens
Nokta Yayılım Fonksiyonu
EMI Koruma

Graphical/Tabular Abstract (Grafik Özet)

The invention of photon sieves and the integration of apodization into these sieves have introduced significant design flexibility in diffractive optical elements (DOEs), enabling the regulation of secondary maxima in the intensity distribution. Unlike conventional methods, this study applies apodization to phase-type photon sieves using metallic structures, which not only adjusts intensity distributions (Figure A a)) but also enhances electromagnetic interference (EMI) shielding (Figure A b)). / Foton eleklerinin icadı ve bu eleklere apodizasyonun entegre edilmesi, kırınımlı optik elemanlarda (DOE'ler) önemli tasarım esnekliği sunarak şiddet dağılımındaki ikincil maksimumların düzenlenmesini sağlamıştır. Geleneksel yöntemlerin aksine, bu çalışma, yalnızca yoğunluk dağılımlarını ayarlamakla kalmayıp (Şekil A a)) aynı zamanda elektromanyetik girişim (EMI) kalkanlamasını da geliştiren (Şekil A b)) metalik yapılar kullanarak faz tipi foton eleklerine apodizasyonu uygular.

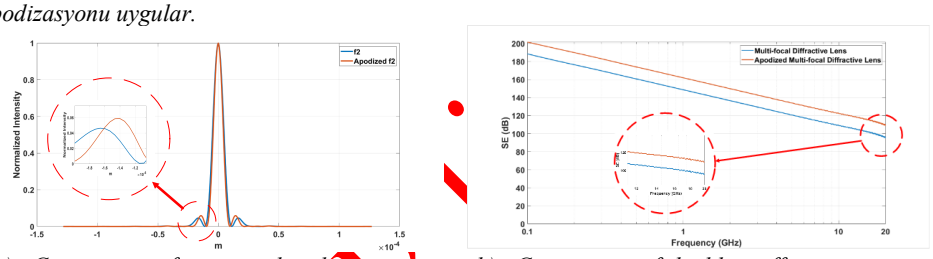

a) Comparison of intensity distributions *b) Comparison of shielding effectiveness*

Figure A: *Comparsion of apodized phase photon sieves with phase photon sieves /* ***Şekil A:*** *Apodize faz foton eleklerinin faz foton elekleri ile karşılaştırılması*

Highlights (Önemli noktalar)

- *Validation of the apodized phase photon sieves by comparison with equivalent phase photon sieves. / Eşdeğer faz foton elekleri ile karşılaştırılarak apodize faz foton eleklerinin doğrulanması.*
- *Comparison of EMI shielding with non-metallic structure. / EMI kalkanlamasının metallik olmayan yapı ile karşılaştırılması.*
- *A novel electro optical system design approach incorporating a two-regional diffractive optical element. / İki bölgeli kırınım optik elemanını bünyesinde barındıran yeni bir elektro-optik sistem tasarım yaklaşımı.*

Aim (Amaç): *This study aims to design an apodized phase photon sieve using metallic structures, which not only regulates secondary maxima but also provides shielding effectiveness in a novel electro-optical system. / Bu çalışmada, metalik yapılar kullanılarak, hem ikincil maksimumları düzenleyen hem de yeni bir elektro-optik sistemde kalkanlama etkinliği sağlayan apodize faz foton eleği tasarımı amaçlanmıştır.*

Originality (Özgünlük): *A novel design methodology for an electro-optical system is introduced, utilizing apodized phase photon sieves with metallic structure for the first time.. / İlk kez metalik yapıya sahip apodize faz foton eleklerini kullanan bir elektro-optik sistem için yeni bir tasarım metodolojisi tanıtılmaktadır.*

Results (Bulgular): *Electromagnetic simulations have demonstrated that apodized phase photon sieves with a metallic structure exhibit improved shielding effectiveness.. / Elektromanyetik simülasyonlar, metalik yapıya sahip apodize faz foton eleklerinin gelişmiş kalkanlama etkinliği sergilediğini göstermiştir.*

Conclusion (Sonuç): *An innovative design approach incorporating apodized phase photon sieves with metallic structure is proposed. The effectiveness of this design was validated through comparative analyses in both optical and electromagnetic bands../ Metalik yapıya sahip apodize faz foton eleklerini içeren yenilikçi bir tasarım yaklaşımı önerilmiştir. Bu tasarımın etkinliği, hem optik hem de elektromanyetik bantlarda karşılaştırmalı analizler yoluyla doğrulanmıştır.*

*Corresponding author, e-mail: ahmetunal.phd@gmail.com
DOI: 10.29109/gujsc.1557933

GU J Sci, Part C, 13(X): XX-XX (2025)

Gazi Üniversitesi
Fen Bilimleri Dergisi
PART C: TASARIM VE TEKNOLOJİ

Gazi University
Journal of Science
PART C: DESIGN AND TECHNOLOGY

http://dergipark.gov.tr/gujsc

Multi-Focal Diffractive Lens by Apodized Phase Photon Sieves

Ahmet ÜNAL[1*]

[1]*Middle East Technical University, Department of Electrical and Electronics Engineering, Ankara, Turkey*

Article Info

Research article
Received: 30/09/2024
Revision: 16/03/2025
Accepted: 24/03/2025

Keywords

Diffractive Optical Elements
Phase Fresnel Zone Plates
Multilevel Diffractive Lens
Point Spread Function
EMI Shielding

Abstract

As a result of the invention of photon sieves and the implementation of apodization to these sieves, significant design freedom has been achieved in diffractive optical elements (DOEs). Thanks to this freedom, secondary maxima in the intensity distribution can be reduced relative to the same photon sieves without apodization.

In this study, unlike traditional methods, applying apodization to phase types of photon sieves using metallic structures is discussed. Thus, not only intensity distributions are adjusted, but also electromagnetic interference (EMI) shielding is achieved. For this purpose, an Apodized Multi-focal Diffractive Lens (AMDL), which can be defined as a hybrid lens, was designed within the scope of this study, and its results were compared with its alternative, Multi-focal Diffractive Lens (MDL). During the design stage, simulations were carried out on two different bands. While the simulations in the optical band were performed using optical wave propagation, the simulations in the RF band were carried out using CST software, and the results were shared. As can be seen from the results, the secondary maxima in the intensity distribution was reduced due to the apodization, and EMI protection was also achieved.

This study will contribute to the development of lenses designed for two different purposes called hybrid lens in this research.

Apodize Faz Foton Elekleri ile Çok Odaklı Kırınımlı Mercek

Makale Bilgisi

Araştırma makalesi
Başvuru: 30/09/2024
Düzeltme: 16/03/2025
Kabul: 24/03/2025

Anahtar Kelimeler

Kırınımlı Optik Eleman
Faz Fresnel Bölge Plakaları
Çok Seviyeli Kırınımlı Lens
Nokta Yayılım Fonksiyonu
EMI Koruma

Öz

Foton eleklerinin icadı ve bu eleklere apodizasyonun uygulanması sonucunda kırınımlı optik elemanlarda (DOE) önemli tasarım özgürlüğü elde edilmiştir. Bu özgürlük sayesinde şiddet dağılımındaki ikincil maksimumlar, apodizasyonsuz aynı foton eleklerine göre azaltılabilmektedir.

Bu çalışmada, geleneksel yöntemlerden farklı olarak, metalik yapılar kullanılarak foton eleklerinin faz tiplerine apodizasyonun uygulanması ele alınmıştır. Böylece, sadece şiddet dağılımları ayarlanmakla kalınmamış, aynı zamanda elektromanyetik girişim (EMI) koruması da sağlanmıştır. Bu amaçla, bu çalışma kapsamında hibrit lens olarak tanımlanabilecek Apodize Çok Odaklı Kırınımlı Lens (AMDL) tasarlanmış ve sonuçları alternatifi Çok Odaklı Kırınımlı Lens (MDL) ile karşılaştırılmıştır. Tasarım aşamasında iki farklı bantta simülasyonlar gerçekleştirilmiştir. Optik banttaki simülasyonlar optik dalga yayılımı kullanılarak gerçekleştirilirken, RF bandındaki simülasyonlar CST yazılımı kullanılarak gerçekleştirilmiş ve sonuçlar paylaşılmıştır. Sonuçlardan da görüleceği üzere, apodizasyon nedeniyle şiddet dağılımındaki ikincil maksimumlar azalmış ve EMI koruması da sağlanmıştır.

Bu çalışma, bu araştırmada hibrit lens olarak adlandırılan iki farklı amaç için tasarlanmış lenslerin geliştirilmesine katkıda bulunacaktır.

1. INTRODUCTION (GİRİŞ)

Due to the high Radio Frequency (RF) transmittance of lens materials in electro-optical systems, EMI shielding is necessary. This shielding is typically provided by metallic structures known as Frequency Selective Surfaces (FSS) in infrared bands or a thin sheet film such as Indium Thin Oxide (ITO) in the visible band. These structures are commonly utilized in electro-optical systems, particularly in the defense industry [1, 2].

With advancements in imaging systems, Diffractive Optical Elements (DOEs) are increasingly replacing conventional refractive optics. When properly designed, DOEs can effectively mitigate optical

*Corresponding author, e-mail: ahmetunal.phd@gmail. com
DOI: 10.29109/gujsc.1557933

aberrations with just one optical element [3-10]. This reduction in the number of optical components not only decreases the weight of the camera but also simplifies optical alignment issues in optical systems. In military and aerial applications [5, 11 - 22], DOEs offer additional advantages by reducing volume and weight, thereby adding flexibility to the design of optical systems. This reduction in volume and weight is particularly beneficial for aerial applications such as cruise missiles and Unmanned Aerial Vehicles (UAVs).

Electro-optical systems employed in military applications require EMI shielding in accordance with the MIL-STD 461 standard (10 kHz - 18 GHz range [23]). Typically, metal coatings formed on flat surfaces of optical components, known as FSSs, are utilized [1, 23-28]. Given that military operations may occur in all-day situations, infrared systems are preferred due to their capability to operate independently of day and night conditions. Additionally, the passive nature of the infrared band and its independence from active sources during operations contribute to their widespread usage. For these reasons, FSS structures are prioritized in infrared systems [23, 24, 28].

As an alternative to periodic unit cell-based FSS structures, a metallic structure with appropriate size and apertures can achieve similar effects in reducing RF transmission. Within the scope of this study, a metallic structure, unlike FSS but providing EMI shielding akin to FSS, is proposed. Besides its application for EMI shielding, the proposed metallic structure is also utilized as an apodization component of phase photon sieves.

2. THEORETICAL BACKGROUND (TEORİK ALTYAPI)

Fresnel Zone Plates (FZPs) comprise concentric rings that alternate between optically opaque and transparent zones. When appropriately designed, each ring contributes to achieving the desired focus [29], making FZP structures function as refractive lenses. Depending on the contribution of the concentric rings to the focus, FZPs can be categorized as Phase FZP (PFZP) and Amplitude FZP (AFZP) [29-33]. PFZP, also known as Multilevel Diffractive Lens [7-10, 34-36], is often preferred in various applications due to its superior diffraction efficiency compared to amplitude types. As a result, they can serve as alternatives to traditional refractive lenses. Amplitude types are less commonly used in applications due to their lower diffraction efficiencies in optical bands. Possible basic types and their calculated diffraction efficiencies of the FZPs are outlined in Table 1.

Table 1. Analytically calculated first-order diffraction efficiencies. (Analitik olarak hesaplanan birinci derece kırınım verimlilikleri)

FZP types	Efficiency (%)
Kinoform (Phase) [37, 38]	100.0
32-Level (Phase) [7, 8, 34, 35, 39]	99.7
16-Level (Phase) [7, 8, 34, 35, 39]	98.7
8-Level (Phase) [7, 8, 34, 35, 39]	95.0
4-Level (Phase) [7, 8, 34, 35, 39]	81.1
2-Level (Phase) [20, 39]	40.5
Sinusoidal (Phase) [39]	33.9
2-Level (Amplitude) [30, 40]	10.1
Sinusoidal (Amplitude) [31-33]	6.25

The study opted for a 4-level PFZP due to its higher diffraction efficiencies compared to amplitude types, despite the availability of higher levels like 8, 16, or 32, or even Kinoform. The decision was influenced by the need to balance computational time and validate the concept of the AMDL with EMI shielding.

The objective of this research is to devise a hybrid lens that mimics the RF behavior of periodic meshed FSS, which minimizes secondary maxima in optical band intensity distribution. To achieve this goal, the study proposes an apodized multi-focal diffractive lens as an alternative to the multi-focal diffractive lens [41].

2.1. Optical Model Of Multilevel Diffractive Lens (Çok Seviyeli Kırınımlı Lensin Optik Modeli)

In scalar diffraction theory, Fresnel and Fraunhofer approximations are well-defined theories that can be applied to many optical systems. Thus, both near and far-field wave distribution can be analyzed analytically or numerically by these approximations. The Huygens Fresnel integral in terms of Fourier Transform under Fresnel approximation is given as follows [42, 43]

$$r(x,y)=\frac{e^{ikd}}{i\lambda d}e^{i\pi\frac{x^2+y^2}{\lambda d}}\Im\left\{u(x',y')e^{i\frac{\pi}{\lambda d}\left((x')^2+(y')^2\right)}\right\}\left(\frac{x}{\lambda d},\frac{y}{\lambda d}\right) \quad (1)$$

The Huygens Fresnel integral in terms of Fourier Transform under Fraunhofer approximation is given as follows [42, 43]

$$r(x,y)=\frac{e^{ikd}}{i\lambda d}e^{i\pi\frac{x^2+y^2}{\lambda d}}\Im\{u(x',y')\}\left(\frac{x}{\lambda d},\frac{y}{\lambda d}\right) \quad (2)$$

where $\Im\{\ \}$ is 2D Fourier Transform, $u(x',y')$ is amplitude distribution in the source plane, $r(x,y)$ is the amplitude distribution in the image plane, d is the distance between the source and image plane, and λ is the wavelength. The geometry of optical wave propagation is given in Figure 1. The Huygens-Fresnel integrals are valid under Fresnel and Fraunhofer approximations. The valid range is defined by the Fresnel number (N_F), and it is given as [44]

$$N_F=\frac{a^2}{\lambda d} \quad (3)$$

where a is the radius of a circular lens aperture. Fresnel number less than 1 indicates that the approximation is suitable, but the Fresnel approximation can still provide good results for Fresnel numbers up to 20 or 30 [44]. When the Fresnel number is much smaller than 1, the Fraunhofer approximation is valid.

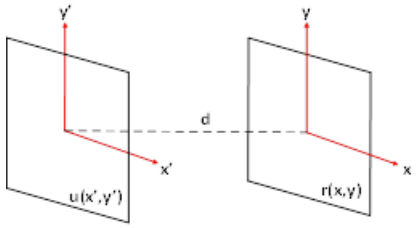

Figure 1. Optical propagation geometry. (Optik yayılma geometrisi.)

In the case of the unit plane wave illumination, the amplitude distribution of the source plane will be the aperture function of the lens just after passing the DOE. Thus, this integral can be written in terms of the Fourier Transform and aperture function of the DOE. This approach makes it possible to apply one-step propagation [45] to the optical propagation geometry. The amplitude distribution in the image plane for Fresnel and Fraunhofer approximations are

$$r(x,y)=\frac{1}{i\lambda d}e^{i\pi\frac{x^2+y^2}{\lambda d}}\Im\left\{A(x',y')_{DOE}e^{i\frac{\pi}{\lambda d}\left((x')^2+(y')^2\right)}\right\}\left(\frac{x}{\lambda d},\frac{y}{\lambda d}\right) \quad (4)$$

$$r(x,y)=\frac{1}{i\lambda d}e^{i\pi\frac{x^2+y^2}{\lambda d}}\Im\{A(x',y')_{DOE}\}\left(\frac{x}{\lambda d},\frac{y}{\lambda d}\right) \quad (5)$$

The exponential phase term is neglected for simplicity. The following equation defines the offered general aperture function of a 4-level DOE.

$$A(x,y)_{DOE}=\sum_{l=1}^{n*L}\exp\left(-i2\pi\frac{l-1/2}{L}\right).\left\{circ\left(\frac{x}{r_l},\frac{y}{r_l}\right)-circ\left(\frac{x}{r_{l-1}},\frac{y}{r_{l-1}}\right)\right\} \quad (6)$$

where n is the number of phase Fresnel zones, L is the number of the subzone, and r_l is the radius of l th subzone. The circular function is

$$circ(x,y)=\begin{cases}1, & if\ \sqrt{x^2+y^2}\le 1\\ 0, & otherwise\end{cases}$$

A schematic representation of the 4-Level PFZP is given in Figure 2.

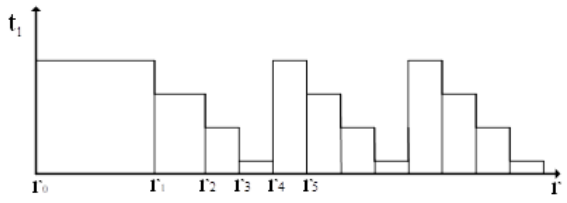

Figure 2. DOE model for 4-Level PFZP. (4-Level PFZP için DOE modeli.)

$$t_l=\frac{(l-1/2)}{L}\frac{\lambda}{(n-1)} \quad (7)$$

where t_l is the thickness of l th subzone, λ is the wavelength, n is the refractive index of the lens material, and 1 is the refractive index of the atmosphere [7, 8, 34, 35]. Theoretically, the

thickness values for each sublevel will change the phase of the plane wave. Therefore, the phases resulting from the thickness are expressed as an exponential product at the beginning of the aperture function. Each subzone can be determined by using the following equation.

$$r_l = \sqrt{\frac{2l\lambda f}{L}} \tag{8}$$

where f is the focal length of the DOE. While simulating the optical propagation, the distance between the source and image plane was taken as the focal length ($d = f$).

Taking into account the Nyquist Sampling criteria [45] in the spatial and spatial frequency domains, to accurately sample the amplitude distribution, 2D grids are defined. The sampling interval of the spatial domain is $\Delta x'$, and the sampling interval in the spatial frequency domain is Δx. The relation between sampling intervals is determined by the Nyquist Sampling criteria and it is given as [45]

$$\Delta x \le \frac{1}{2\Delta x'} \tag{9}$$

The amplitude distribution can be written in terms of sampling intervals in spatial and spatial frequency domains. The intensity distribution is the absolute square of the amplitude distribution. The sampled versions are

$$I(m,n) = \left| \frac{1}{i\lambda d} e^{i\pi\lambda d\left(m^2\Delta x^2 + n^2\Delta x^2\right)} \cdot \Im\left\{ A(m\Delta x', n\Delta x')_{DOE}\, e^{i\frac{\pi}{\lambda d}\left(m^2(\Delta x')^2 + n^2(\Delta x')^2\right)} \right\} \right|^2 \tag{10}$$

$$I(m,n) = \left| \frac{1}{i\lambda d} e^{i\pi\lambda d\left(m^2\Delta x^2 + n^2\Delta x^2\right)} \Im\left\{ A(m\Delta x', n\Delta x')_{DOE} \right\} \right|^2 \tag{11}$$

2.2. Optical Model of Multi-Focal Diffractive Lens (MDL)

(Çok Odaklı Kırınımlı Lensin (MDL) Optik Modeli)

MDL consists of two regions. The first region, the central part of the lens, is the first focal length, and the second region, the outer part of the lens, is the second focal length. In each region (central and outer), parameters required to determine the aperture functions are calculated separately according to focal length, wavelength, and the number of phase Fresnel zones. Therefore, the total aperture function is the sum of the aperture functions. The aperture function of the first region ($A_{f1}(x,y)$) is

$$A_{f1}(x,y) = \sum_{l=1}^{n*L} \exp\left(-i2\pi \frac{l-1/2}{L}\right) \cdot \left\{ circ\left(\frac{x}{r_l}, \frac{y}{r_l}\right) - circ\left(\frac{x}{r_{l-1}}, \frac{y}{r_{l-1}}\right) \right\} \tag{12}$$

The aperture function of the second region ($A_{f2}(x,y)$) is

$$A_{f2}(x,y) = \left[1 - circ\left(\frac{x}{r_{out}}, \frac{y}{r_{out}}\right)\right] .* \left[\sum_{l=1}^{n*L} \exp\left(-i2\pi \frac{l-1/2}{L}\right) \cdot \left\{ circ\left(\frac{x}{r_l}, \frac{y}{r_l}\right) - circ\left(\frac{x}{r_{l-1}}, \frac{y}{r_{l-1}}\right) \right\} \right] \tag{13}$$

The final Aperture function will be the combination of aperture functions, and it can be defined as

$$A_{MDL}(x,y) = A_{f_1} + A_{f_2} \tag{14}$$

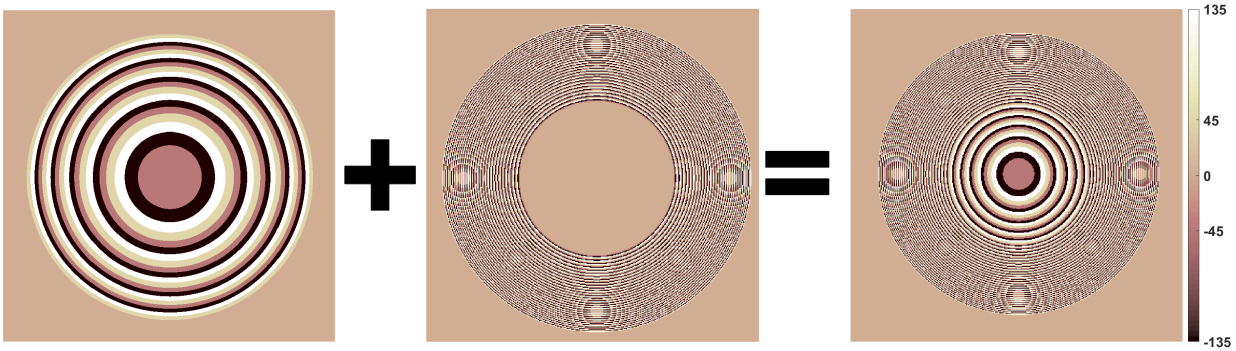

Figure 2. Aperture functions of MDL in terms of complex angles. The unit of the graphs is in degrees.
(Karmaşık açılar cinsinden MDL'nin açıklık fonksiyonları. Grafiklerin birimi derecedir.)

2.3. Optical Model Of Multi-Focal Diffractive Lens (MDL)

(Çok Odaklı Kırınımlı Lensin (MDL) optik modeli)

The aperture function of the first region ($A_{f1}(x,y)$) is the same as with the MDL. However, the outer region has to be different in order to decrease the secondary maxima, and apodization has to be applied. The apodization can also be applied to not only amplitude types of photon sieves but also the phase photon sieves. In the literature, there are many apodized types such as Bartlett, Blackman, Connes, Gaussian, etc. [46]. Since this study is based on the application of apodization to phase photon sieves using metallic structures, any type of apodization is sufficient. For this reason, Gaussian apodization was chosen. The aperture function of the outer region is

$$A_{Af2}(x,y)=\sum_{l=21}^{n*L}\left(\sum_{n=1}^{N_l}\exp\left(-i2\pi\frac{l-1/2}{L}\right).\operatorname{circ}\left(\frac{x-c}{d_l},\frac{y-y_n}{d_l}\right)\right) \quad (15)$$

The Gaussian apodization function [46, 47] is

$$N_l=\left\lfloor\frac{\pi r_l}{2d_l}.\exp\left(-2\frac{r_l^2}{r_{out,f2}^2}\right)\right\rfloor \quad (16)$$

N_l is the number of phase sieves in each subzone level, $r_{out,f2}$ is the outermost sublevel radius of the second region, d_l is the radius of the sieves in l^{th} subzone, and x_n , y_n values are the central location of the sieves. The first term in equation (16) gives the total number of sieves after it is multiplied by the Gaussian apodization function [47]. Here, $\lfloor . \rfloor$ operator represents the lower ceiling operation. In this way, the number of sieves in each region is determined, and they are distributed symmetrically. After each aperture function of the first and second focal length is calculated separately, the total aperture function will be the sum of the individual aperture functions.

$$A_{AMDL}(x,y)=A_{f_1}+A_{Af_2} \quad (17)$$

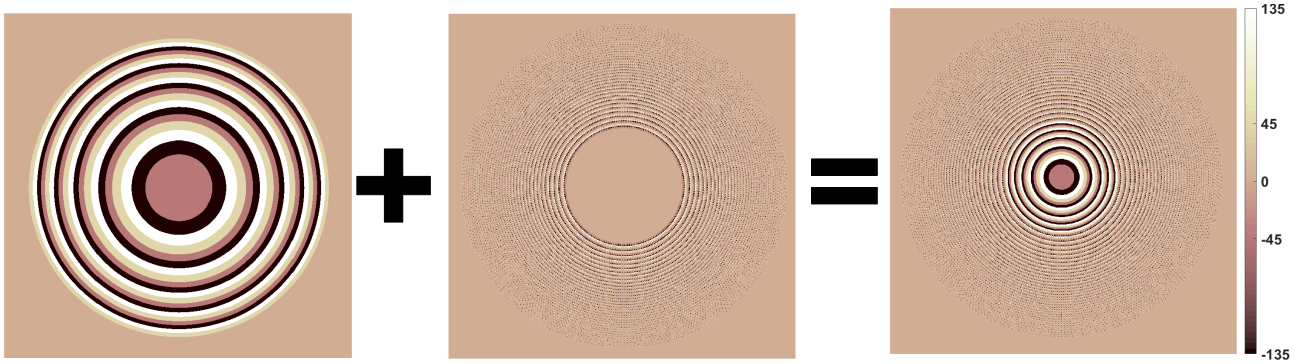

Figure 4. Aperture function of AMDL in terms of complex angles. (Kompleks açılar cinsinden AMDL'nin açıklık fonksiyonu.)

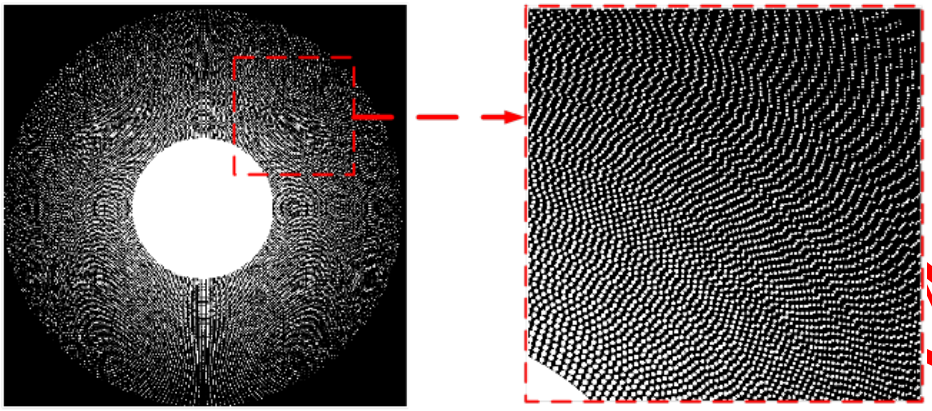

a) Aperture function of the AMDL in terms of magnitude. (AMDL'nin açıklık fonksiyonu büyüklük cinsinden)

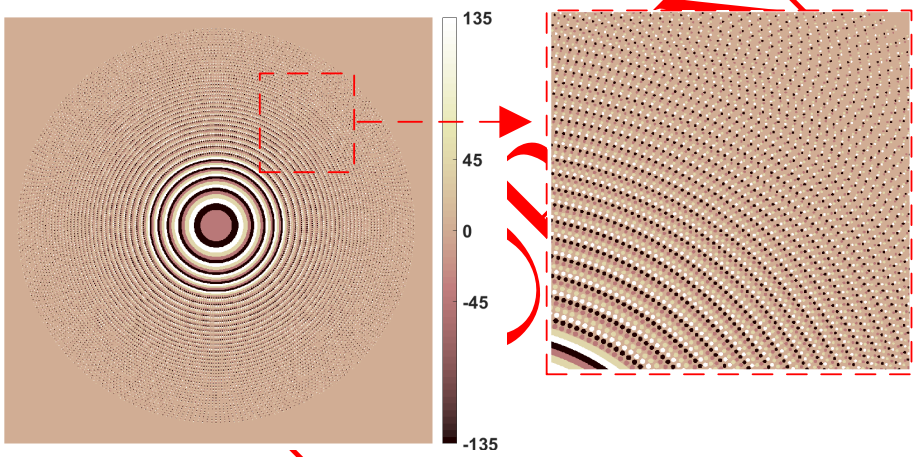

b) The aperture function of the AMDL in terms of imaginary angles (the unit of the graphs is in degrees) (AMDL'nin sanal açılar cinsinden açıklık fonksiyonu (Grafiklerin birimi derecedir))

Figure 5. Aperture function of the AMDL. (AMDL'nin açıklık fonksiyonu.)

2.4. Electromagnetic Model Of Diffractive Lenses

(Kırınımlı Lenslerin Elektromagnetik Modeli)

Shielding effectiveness is a measure of an enclosure how the incident wave is transmitted, and it is defined as the ratio of the incident wave (E_i) to the transmitted wave (E_t). Shielding effectiveness (SE_{linear}) is given with the following equation [1, 2]

$$SE_{linear} = \frac{E_i}{E_t} \tag{18}$$

Shielding effectiveness in dB unit is [1, 2]

$$SE_{dB} = 20 log_{10}\left(SE_{linear}\right) \tag{19}$$

Under the unit plane wave illumination, the SE can be defined as follows.

$$SE_{dB} = 20 log_{10}\left(\frac{1}{E_t}\right) = -E_{t,dB} \tag{20}$$

CST model for electromagnetic simulations of metallic enclosures is given in Figure 6 with two perfect conductor (PEC) structures, and boundary conditions were chosen as perfectly matched layers

(PML) [2]. A uniform plane wave at normal incidence excites the structures. The contribution of the lens material to the shielding effectiveness has been neglected in the models. So the simulations were performed separately for each structure without the diffractive lens. The Electric Field data is generated at the far-field (3 m) and, SE is calculated using the SE_{dB} equation (20).

The first model given in Figure 6 is the model of the circular aperture with the same diameter as the diffractive lens. The second model is proposed for metallic structured AMDL.

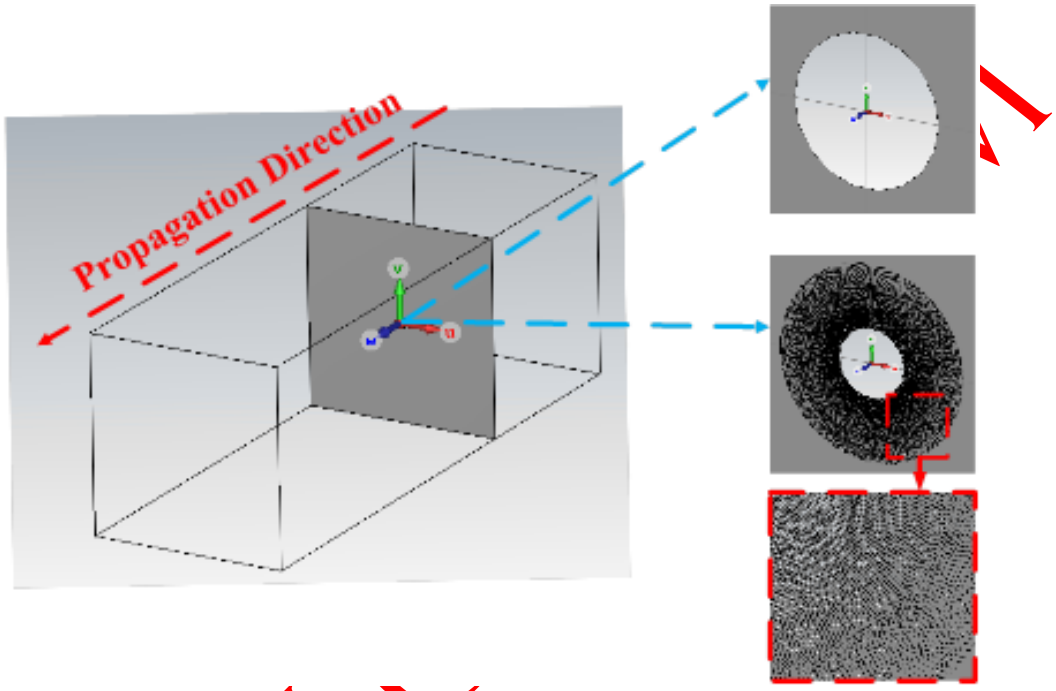

Figure 6. An overview of the CST model of the AMDL and MDL (AMDL ve MDL'nin CST modeline genel bakış)

3.SIMULATIONS AND RESULTS (SİMÜLASYONLAR ve BULGULAR)

The simulations were carried out in two different bands in the electromagnetic spectrum. First, due to the restriction coming from the MIL-STD 461 standard, the behavior of hybrid structures when exposed to RF was simulated between 100 MHz and 18 GHz using CST electromagnetic simulation software.

Second, since the military applications are considered, simulations were performed in the infrared band at 1064 nm wavelength. The first focal length is simulated in the visible band at 638 nm. The simulations can also be performed at different wavelengths or bands. However, only 1064 nm and 638 nm were preferred in this study for simplicity.

3.1. Electromagnetic Simulations (Elektromagnetik Simülasyonlar)

As a result of the CST simulations, AMDL has an advantage in protecting the electro-optical system. The difference between the MDL and AMDL is 13.7 dB. The shielding performance of the AMDL is better than the MDL.

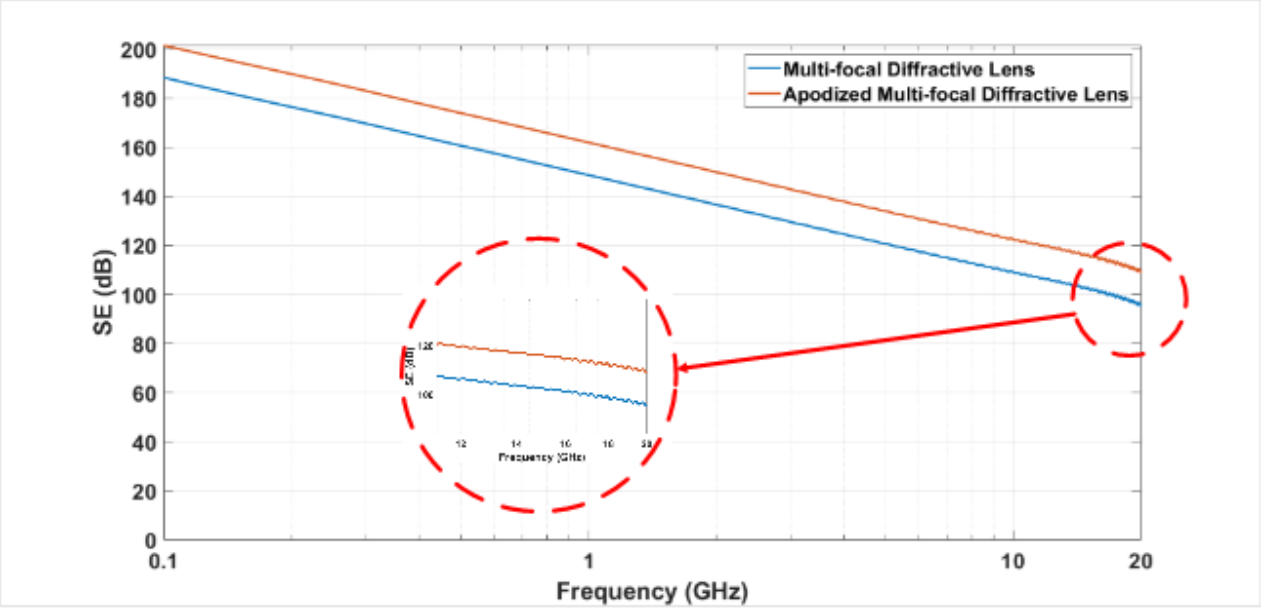

Figure 7. SE calculation results for the structures (Yapılar için SE hesaplama sonuçları)

3.2. Optical Simulations (Optik Simülasyonlar)

After determining the sampling parameters of the proposed aperture functions and Huygens-Fresnel Integrals, optical wave propagated [45] for the two apertures as shown in Fig 8. using equations (10) and (11). The results are presented in Figure 9 a) and b). Optical parameters of the MDL and AMDL are given in Table 2 and Table 3. The simulations are completed at the level of seconds after the aperture functions were defined.

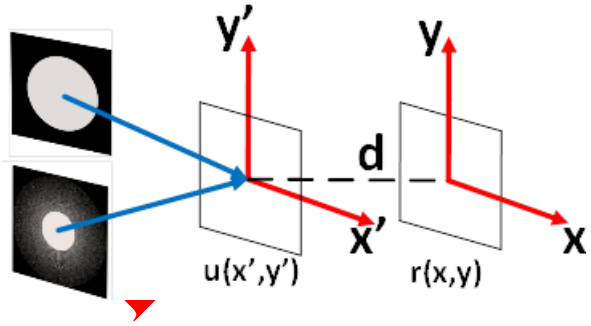

Figure 8. Optical propagation geometry for the aperture functions (A_{AMDL} , A_{MDL}) (Açıklık fonksiyonları için optik yayılma geometrisi (A_{AMDL} , A_{MDL}))

For the validity of the Fraunhofer approximation to be acceptable, the quadratic phase term should be small enough in the Huygens Fresnel integrals. Otherwise, the Fresnel approximation is logical. To be sure about the validity of the Fraunhofer approximation, the following calculation can be done. After that, for phase photon sieves, the Fraunhofer approximation was used in optical propagation.

$$d >> \frac{\pi d_1^{\,2}}{\lambda} \Rightarrow \begin{cases} f_2 >> \dfrac{\pi d_{21}^{\,2}}{\lambda_2} \Rightarrow 24 >> 0.14 \quad for\ d_{21} = 5.422\mu m \\ f_2 >> \dfrac{\pi d_{120}^{\,2}}{\lambda_2} \Rightarrow 24 >> 0.02 \quad for\ d_{120} = 2.022\mu m \end{cases}$$

Table 2. Optical parameters of MDL (MDL'nin optik parametreleri)

	Parameters	Value
Central Region	Focal length (f_1)	24 mm
	Diameter	1 mm
	Wavelength (λ_1)	1.064 nm
	Number of Phase Fresnel Zones	5
	Fresnel Number (N_F)	10
Outer Region	Focal Length (f_2)	40 mm
	Diameter	~ 3 mm
	Wavelength (λ_2)	638 nm
	Number of Phase Fresnel Zones	5 - 40
	Fresnel Number (N_F)	80

Table 3. Optical parameters of AMDL (AMDL'nin optik parametreleri)

	Parameters	Value
Central Region	Focal length (f_1)	24 mm
	Diameter	1 mm
	Wavelength (λ_1)	1.064 nm
	Number of Phase Fresnel Zones	5
	Fresnel Number (N_F)	10
Outer Region	Focal Length (f_2)	40 mm
	Diameter	~ 3 mm
	Wavelength (λ_2)	638 nm
	Number of Phase Fresnel Zones	5 - 40
	Fresnel Number (N_F)	80

The simulation results show that the proposed hybrid structure minimizes the secondary maxima in the intensity distribution of the second focal length. Normalized intensity values of the MDL are shown in Figure 9 a) and normalized intensity values of AMDL are shown in Figure 9 a). For better observation, the difference is shown in Figure 10.

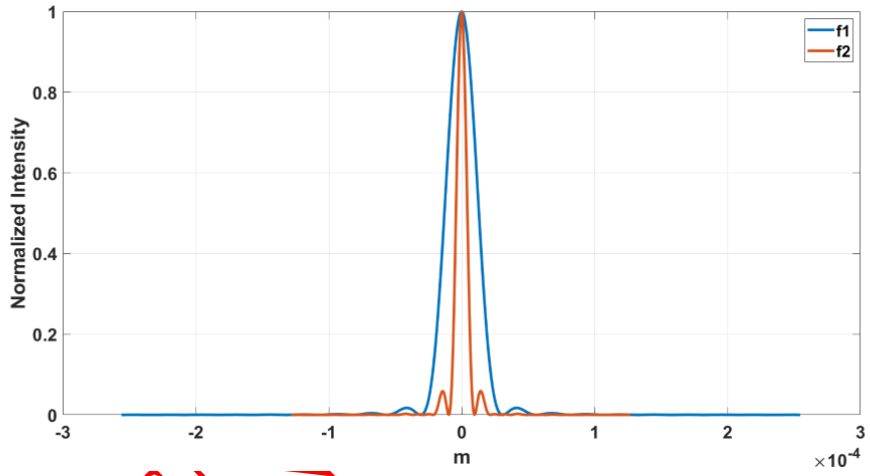

a) Cross section of normalized intensity distributions of the MDL (MDL'nin normalleştirilmiş şiddet dağılımlarının kesiti.)

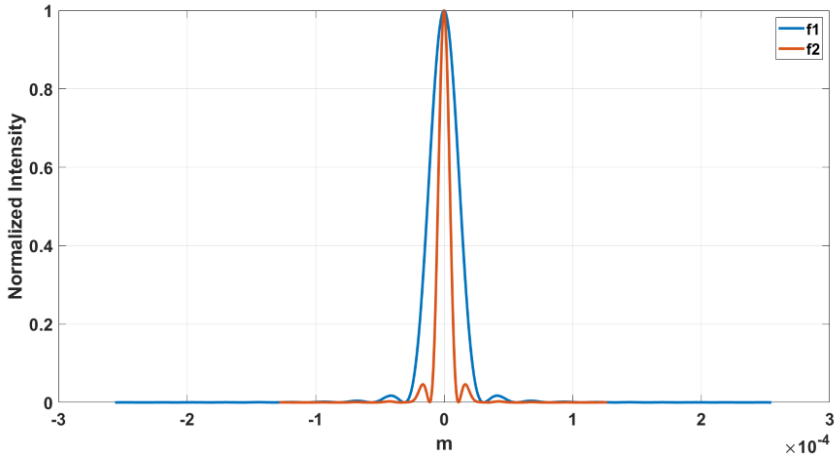

b) Cross section of normalized intensity distributions of the AMDL (AMDL'nin normalleştirilmiş şiddet dağılımlarının kesiti.)

Figure 9. Simulation results of MDL and AMDL. (MDL ve AMDL'nin simülasyon sonuçları)

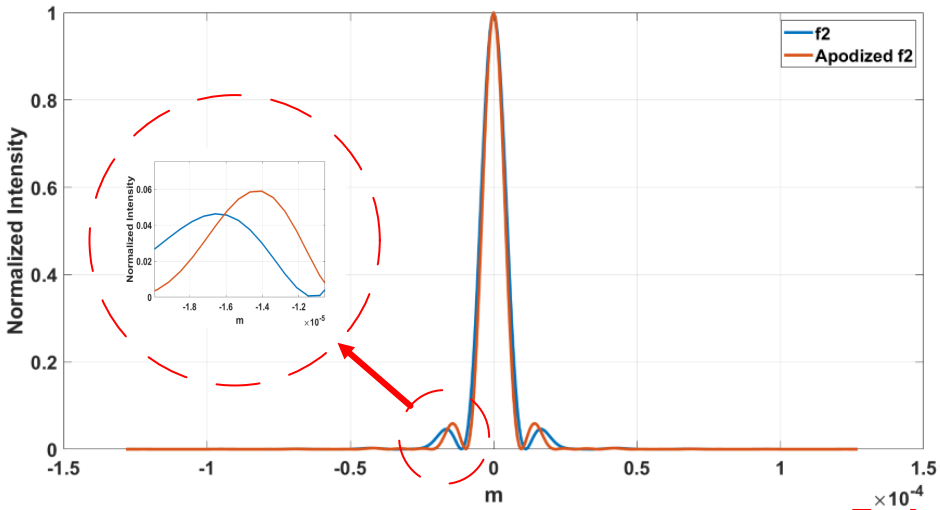

Figure 10. Comparison of AMDL and MDL. (MDL ve AMDL'nin karşılaştırılması)

A single-lens system with two focal lengths enables the effective integration of two electro-optical systems operating in different spectral bands through a common aperture optical design approach. Fig. 11 illustrates the system's operational potential. The first focal length is designed for a wavelength commonly used in laser spot tracker systems. However, if the application requires a laser rangefinder, the design wavelength can be adjusted to 1550 nm instead of 1064 nm.

The second focal length, designed for 638 nm, refers to the visible spectrum. The design for the visible band was carried out for only one wavelength. In this study, the visible band design is optimized for a single wavelength, but a complete design must account for all wavelengths within the visible range (400–700 nm), requiring further optimization.

The approach proposed in this study facilitates the development of an electro-optic system that integrates both a laser system and a visible sensor within a common aperture optical design. While this study primarily focuses on the visible band and laser wavelengths to validate the design, the same methodology can be extended to laser wavelengths and the infrared spectrum, including long-wave infrared (LWIR) and mid-wave infrared (MWIR) [1, 14, 15, 17, 18, 39, 48-51].

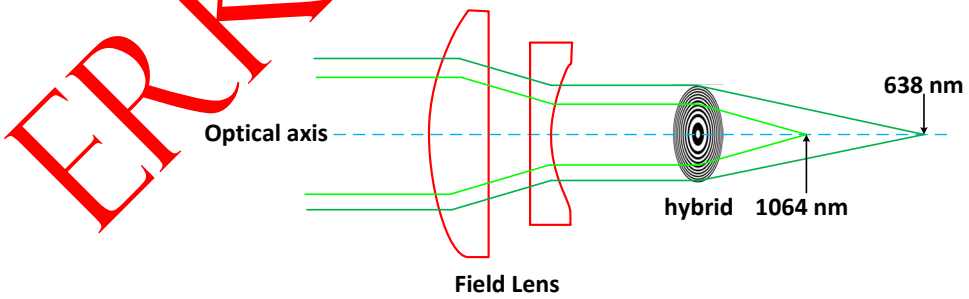

Figure 11. Illustration of an electro-optic system using the two-foci diffractive lens system (İki odaklı kırınımlı mercek sistemi kullanan bir elektro-optik sistemin gösterimi)

Apodization involves adjusting the pinhole density on each ring of the photon sieve to create a smooth transmission window, thereby enhancing the suppression of secondary maxima in a diffraction pattern. Gaussian apodization was selected as the preferred method; however, other techniques such as Bartlett, Blackman, Connes, Cosine, Hamming, Hanning, etc., are also available. For a diffractive

lens designed to operate at two focal lengths and two wavelengths, each apodization method can be analyzed individually, and if necessary, an additional window function can be incorporated. Evaluating and selecting the apodization technique that yields the best results across all wavelengths not for a single wavelength in the spectrum would further enhance optical performance [52, 53]. Because of this reason, the optimum apodization technique was not determined during the simulation of the hybrid structure. It must be determined for all wavelengths within the imager's spectral sensitivity.

4. CONCLUSION (SONUÇ)

This research found that the proposed AMDL minimizes the secondary maxima in the intensity distribution of the second focal length. The hybrid AMDL is offered as an alternative way to the MDL lens, and also, the apodization has been added to the lens with the help of a metallic structure. Thus, the hybrid structure is proposed for military applications where the use of FSS is necessary, and better in optical and RF bands. From this point of view, secondary maxima in the intensity values of the AMDL were eliminated in the optical band. An alternative way of protecting the optical system from EMI was accomplished. In this way, the hybrid structure, which provides benefits in both RF and optical bands, was proposed.

This research will contribute to the development of hybrid structures in optical and RF bands of the electromagnetic spectrum. This study can also be extended for any diffractive achromat instead of a single wavelength diffractive lens with a similar approach stated in this research.

DECLARATION OF ETHICAL STANDARDS (ETİK STANDARTLARIN BEYANI)

The author of this article declares that the materials and methods they use in their work do not require ethical committee approval and/or legal-specific permission.

Bu makalenin yazarı çalışmalarında kullandıkları materyal ve yöntemlerin etik kurul izni ve/veya yasal-özel bir izin gerektirmediğini beyan ederler.

AUTHORS' CONTRIBUTIONS (YAZARLARIN KATKILARI)

Ahmet ÜNAL: He conducted the simulations, analyzed the results and performed the writing process.

Simülasyonları yapmış, sonuçlarını analiz etmiş ve maklenin yazım işlemini gerçekleştirmiştir.

CONFLICT OF INTEREST (ÇIKAR ÇATIŞMASI)

There is no conflict of interest in this study.

Bu çalışmada herhangi bir çıkar çatışması yoktur.

REFERENCES (KAYNAKLAR)

[1] A. Ünal, (2023), "Frequency selective diffractive optical element (FSDOE)", Proc. SPIE 12518, Window and Dome Technologies and Materials XVII, 125180C; https://doi.org/10.1117/12.2657048

[2] N. B. Mentesana, (2011), "Characterization of shielding effectiveness for metallic enclosures" Masters Theses. 4964. https://scholarsmine.mst.edu/masters_theses/4964

[3] T. Grulois, G. Druart, N. Guérineau, A. Crastes, H. Sauer, and P. Chavel, (2014), "Extra-thin infrared camera for low-cost surveillance applications" Opt. Lett. 39, 3169-3172 http://dx.doi.org/10.1364/OL.39.003169

[4] S. Banerji, M. Meem, A. Majumder, F. G. Vasquez, B. S.-Rodriguez, and R. Menon, (2019), "Ultra-thin near infrared camera enabled by a flat multi-level diffractive lens" Opt. Lett. 44, 5450-5452

[5] W. Zhang, B. Zuo, S. Chen, H. Xiao, and Z. Fan, (2013), "Design of fixed correctors used in conformal optical system based on diffractive optical elements" Appl. Opt. 52, 461-466

[6] H.-J. Niu, J. Zhang, A-q. Yan, H.-b. Leng, J.-q. Fei, D.-s. Wu, J.-z. Cao, (2015), "Optical system design for wide-angle airborne mapping camera with diffractive optical element," Proc. SPIE 9449, The International Conference on Photonics and Optical Engineering (icPOE 2014), 94492N doi: 10.1117/12.2085042

[7] Y. Peng, Q. Fu, H. Amata, S. Su, F. Heide, and W. Heidrich, (2015), "Computational imaging using lightweight diffractive-refractive optics" Opt. Express 23, 31393-31407

[8] Y. Peng, (2018), "Computational Imaging with Diffractive Optics", A Thesis Submitted In Partial Fulfillment Of The Requirements For the Degree Of Doctor Of Philosophy, The University of British Columbia April DOI : 10.14288/1.0365608

[9] Y. Peng, Q. Fu, F. Heide, W. Heidrich, (2016), "The Diffractive Achromat: Full Spectrum Computational Imaging with

Diffractive Optics" ACM Trans. Graph. 35, 4, Article 31 (July 2016), https://doi.org/10.1145/2897824.2925941

[10] P. Wang, N. Mohammad, & R. Menon, (2016), "Chromatic-aberration-corrected diffractive lenses for ultra-broadband focusing." Sci Rep 6, 21545 https://doi.org/10.1038/srep21545

[11] J. P. Mills, (2001), "Conformal optics: theory and practice" Proc. SPIE 4442, Novel Optical Systems Design and Optimization IV, doi:10.1117/12.449962

[12] R. R. Shannon, (1999), "Overview of conformal optics," Proc. SPIE 3705, Window and Dome Technologies and Materials VI, doi: 10.1117/12.354622

[13] M. Hinnrichs, B. Hinnrichs, E. McCutchen, (2017), "Infrared hyperspectral imaging miniaturized for UAV applications," Proc. SPIE 10177, Infrared Technology and Applications XLIII, 101770H doi: 10.1117/12.2262125

[14] A. Ünal, (2023), "Semi-active laser seeker design with combined diffractive optical element (CDOE)". J Opt 52, 956–968 https://doi.org/10.1007/s12596-022-00954-5

[15] A. Ünal, (2023), "Laser seeker design with multi-focal diffractive lens", Eng. Res. Express 5 045014, DOI 10.1088/2631-8695/ad0024

[16] T Ren, T Jiao, X. Ling, L. Hu, S. Zhu, (2020), "Design and analysis of distributed semi-active laser detection system," Proc. SPIE 11455, Sixth Symposium on Novel Optoelectronic Detection Technology and Applications, 114554O doi: 10.1117/12.2564981

[17] A. Ünal, (2024), "Dual mode, imaging infrared and semi-active laser, seeker design with squinted combined diffractive optical element". J Opt https://doi.org/10.1007/s12596-024-01657-9

[18] A. Ünal, (2024). Electro-optical system, imaging infrared and laser range finder, design with dual squinted combined lens for aerial targets. Journal of Optics (India), https://doi.org/10.1007/s12596-024-02057-9

[19] K. Qian, T. Li, J. Li, (2018), "Design of a semi-active laser/active radar/ infrared common aperture compound optical system," Proc. SPIE 10832, Fifth Conference on Frontiers in Optical Imaging Technology and Applications, 108321H doi: 10.1117/12.2511609

[20] Q. Huang, B. Lang, L. Xue, (2019), "Design of strapdown laser guided seeker," Proc. SPIE 11023, Fifth Symposium on Novel Optoelectronic Detection Technology and Application, 1102350 doi: 10.1117/12.2520601

[21] J. Barth, A. Fendt, R. Florian, W. Kieslich, (2007), "Dual-mode seeker with imaging sensor and semi-active laser detector," Proc. SPIE 6542, Infrared Technology and Applications XXXIII, 65423B doi: 10.1117/12.719571

[22] X. Zhang, Z. Yang, T. Sun, H. Yang, K. Han, B. Hu, (2017), "Optical system design with common aperture for mid-infrared and laser composite guidance," Proc. SPIE 10256, Second International Conference on Photonics and Optical Engineering, 102560S doi: 10.1117/12.2256433

[23] K. T. Jacoby, M. W. Pieratt, J. I. Halman, K. A. Ramsey, (2009), "Predicted and measured EMI shielding effectiveness of a metallic mesh coating on a sapphire window over a broad frequency range" Proc. SPIE 7302, window and Dome Technologies and Materials XI, 73020X doi: 10.1117/12.818200

[24] M. Yu, N. Xu, H. Liu, and J. Gao, (2014), "Infrared transparent frequency selective surface based on metallic meshes" AIP Advances 4, 027112 https://doi.org/10.1063/1.4866292

[25] Z. Lu, J. Tan, J. Qi, Z. Fan, L. Zhang, (2011), "Modeling Fraunhofer diffractive characteristics for modulation transfer function analysis of tilted ring metallic mesh", Optics Communications 284 3855–3861, doi:10.1016/j.optcom.2011.04.040

[26] A. A. Dewani, S. G. O'Keefe, D. V. Thiel, and A. Galehdar, (2015), "Optically transparent frequency selective surfaces on flexible thin plastic substrates", AIP Advances 5, 027107 https://doi.org/10.1063/1.4907929

[27] Z. Lu, Y. Liu, H. Wang, Y. Zhang, and J. Tan, (2016), "Optically transparent frequency selective surface based on nested ring metallic mesh", Vol. 24, No. 23 OPTICS EXPRESS 26109

[28] Y.-J. Sun, H. Chang, S.-h. Wu, Y.-B. Leng & L. Wang, (2015) "Study on Electromagnetic Shielding of Infrared /Visible Optical Window", Modern Applied Science; Vol. 9, No. 13;, doi:10.5539/mas.v9n13p231

[29] A. Ünal, (2025), Numerical Fresnel models of Fresnel zone plates for plane wave at angle of incidence, Sci Rep 15, 9246 https://doi.org/10.1038/s41598-025-92965-y

[30] D. Atwood, (2000) Soft X-Rays and Extreme Ultraviolet, Cambridge University Press,

[31] H. Jeong, H. Shin, S. Zhang, X. Li and S. Cho (2019), "Application of Fresnel Zone Plate Focused Beam to Optimized Sensor Design for Pulse-Echo Harmonic Generation Measurements", Sensors 19, 1373; doi:10.3390/s19061373

[32] M. M. Greve, A. M. Vial, J. J. Stamnes, and B. Holst, (2013), "The Beynon Gabor zone plate: a new tool for de Broglie matter waves and hard X-rays? An off axis and focus intensity investigation," Opt. Express 21, 28483-28495

[33] H. Zhang, J. C. Li, D. W. Doerr, and D. R. Alexander, (2006), "Diffraction characteristics of a Fresnel zone plate illuminated by 10 fs laser pulses," Appl. Opt. 45, 8541-8546

[34] Y. Zhang, J. Chen, X. Yea, (2007), "Multilevel phase Fresnel zone plate lens as a near-field optical element", Elsevier, Optics Communications 269 271–273, DOI:10.1016/j.optcom.2006.08.006

[35] Y.-JuZhang, C.-W. Zheng, H.-C. Xiao, (2005), "Improving the resolution of a solid immersion lens optical system using a multiphase Fresnel zone plate", Elsevier Optics & Laser Technology 37 444–448, https://doi.org/10.1016/j.optlastec.2004.07.011

[36] Z. Zhang, C. Guo, R. Wang, H. Hu, X. Zhou, T. Liu, D. Xue, X. Zhang, F. Zhang, and X. Zhang, (2017), "Hybrid-level Fresnel zone plate for diffraction efficiency enhancement," Opt. Express 25, 33676-33687, https://doi.org/10.1364/OE.25.033676

[37] L. N. Hazra, Y. Han, C.A. Delisle, Kinoform lenses: (1995), "Sweatt model and phase function", Optics Communications, Volume 117, Issues 1–2, Pages 31-36, https://doi.org/10.1016/0030-4018(95)00071-F

[38] L. Hazra and C. A. Delisle, (1997), "Higher order kinoform lenses: diffraction efficiency and aberrational properties," Optical Engineering 36(5), https://doi.org/10.1117/1.601375

[39] A. Ünal, (2024), "Analytical and numerical fresnel models of phase diffractive optical elements for imaging applications.", Opt Quant Electron 56, 960 https://doi.org/10.1007/s11082-024-06906-6

[40] M M. Howells, C. Jacobsen, T. Warwick, A. V. Bos, (2007) Principles and applications of zone plate x-ray microscopes, Springer Science+Business Media, LLC https://doi.org/10.1007/978-0-387-49762-4_13,

[41] W. A. Britton, Y. Chen, F. Sgrignuoli, L. D. Negro, (2021), "Compact Dual-Band Multi-Focal Diffractive Lenses", https://doi.org/10.1002/lpor.202000207

[42] J. W. Goodman, (1996), Introduction to Fourier Optics, Second Edition, McGraw-Hill Series

[43] R. E. Blahut, (2004), Theory of Remote Image Formation, Cambridge University Press

[44] T. W. N. Dickinson, (2016), "Simulation, Design, and Test of Square, Apodized Photon Sieves for High-Contrast, Exoplanet Imaging" Theses and Dissertations. https://scholar.afit.edu/etd/336

[45] J. D. Schmidt, (2010), "Numerical Simulation of Optical Wave Propagation With examples in MATLAB", SPIE Press

[46] G. Cheng, T. Xing, Z. Liao, Y. Yang, J. Ma, (2008), "Resolution enhancement of photon sieve based on apodization" Proc. SPIE 6832, Holography and Diffractive Optics III, 683229 doi: 10.1117/12.756787

[47] T. Liu, L. Wang, J. Zhang, Q. Fu, And X. Zhang (2018), "Numerical simulation and design of an apodized diffractive optical element composed of open-ring zones and pinholes", Vol. 57, No. 1 / Applied Optics, https://doi.org/10.1364/AO.57.000025

[48] A. Ünal, (2014), "Imaging infrared seeker design," M.S. Master of Science, Middle East Technical University, https://hdl.handle.net/11511/23647

[49] G. G. Artan and H. Sari, (2017) "Design of a cost-effective laser spot tracker", Proc. SPIE 10191, Laser Radar Technology and Applications XXII, 1019107 https://doi.org/10.1117/12.2262343

[50] D.-L. Kim, H.-B. Kong, and S.-T. Lee, (2021) "Effects of solar noise on the detection range performance of a laser spot tracker," Optical Engineering 60(3),

037102. https://doi.org/10.1117/1.OE.60.3.037102

[51] Ünal, A. (2025). Common Aperture DSLR Camera Design Approach with Diffractive Lens. Gazi Üniversitesi Fen Bilimleri Dergisi Part C: Tasarım Ve Teknoloji1-1. https://doi.org/10.29109/gujsc.1564503

[52] Hsiu-Hsin Chung, "Fabrication and Testing Of Dual-Wavelength Photon Sieves", University Of Florida, University Of Florida, Doctorate Thesis, 2005

[53] Dickinson, Thomas W.N., "Simulation, Design, and Test of Square, Apodized Photon Sieves for High-Contrast, Exoplanet Imaging" (2016).Theses and Dissertations. 336. https://scholar.afit.edu/etd/33